physica status solidi

www.interscience.wiley.com

reprints

www.pss-rrl.com

www.pss-c.com

www.pss-b.com

www.pss-a.com

WILEY-VCH

Phys. Status Solidi C **6**, No. 11, 2367–2369 (2009) / **DOI** 10.1002/pssc.200982063

physica status solidi c
www.pss-c.com
current topics in solid state physics

Quenched-in vacancies in Fe-Al alloys

Oksana Melikhova[*,1], Jakub Cizek[1], Ivan Prochazka[1], Jan Kuriplach[1], Frantisek Lukac[1], Miroslav Cieslar[1], Gerhard Brauer[2], and Wolfgang Anwand[2]

[1] Faculty of Mathematics and Physics, Charles University in Prague, V. Holesovickach 2, 180 00 Praha 8, Czech Republic
[2] Institut für Ionenstrahlphysik und Materialforschung, Forschungszentrum Dresden-Rossendorf, Postfach 510119, 01314 Dresden, Germany

Received 15 January 2009, revised 12 March 2009, accepted 02 April 2009
Published online 5 October 2009

PACS 61.50.Nw, 61.72.jd, 78.70.Bj

[*] Corresponding author: e-mail oksivmel@yahoo.com, Phone: +42 221 912 788, Fax: +42 221 912 567

Quenched-in vacancies in Fe_3Al-based intermetallics were studied in this work. A stoichiometric Fe_3Al alloy was compared with non-stoichiometric specimens either with a deficiency or with an excess in Al content. Vacancies in specimens quenched from the disordered A2 phase were investigated by three independent techniques of positron annihilation spectroscopy: positron lifetime (LT) studies, slow positron implantation spectroscopy (SPIS) with a continuous slow positron beam, and coincidence Doppler broadening (CDB). It was found that the combination of LT and SPIS enables to determine reliably even very high concentrations of vacancies. Infor-mation about the local chemical environment of quenched-in vacancies was obtained from CDB measurements.

1 Introduction Intermetallics based on Fe_3Al exhibit a number of features advantageous for structure applications: a low density, a high strength, and a good corrosion resistance. A very interesting property of Fe_3Al-based alloys is a low formation energy of vacancies. The equilibrium concentration of thermal vacancies observed in Fe_3Al-based alloys at high temperatures appears to be as high as several at.% [1]. By quenching from elevated temperatures, a high concentration of non-equilibrium vacancies can be retained at room temperature.

Characterization of quenched-in vacancies in Fe_3Al-based alloys was performed in this work. A stoichiometric Fe_3Al alloy was compared with non-stochiometric specimens either with a deficiency or with an excess in Al content. Defect studies were performed by three independent techniques of positron annihilation spectroscopy, namely positron lifetime (LT) studies, slow positron implantation spectroscopy (SPIS) on a continuous slow positron beam, and coincidence Doppler broadening (CDB).

2 Experimental The following materials were studied in the present work: (i) an Fe_3Al alloy with the stoichiometric composition, (ii) an $Fe_{75.99}Al_{24.01}$ alloy with an under-stoichiometric Al content, and (iii) an over-stoichiometric $Fe_{71.98}Al_{28.02}$ alloy. Studied alloys were annealed at 1000°C for 1h in vacuum (10^{-3} mbar) encapsulated in silicon glass ampoules. The annealing treatment was finished by quenching of the silicon glass ampoule into water of room temperature. As the annealing was performed in the disordered A2 phase region, it is expected that A2 is at least partially retained in the quenched samples. However domains transferred into the B2 phase and the ordered $D0_3$ phase are present in the quenched samples as well. A well annealed pure α-Fe (99.99%) and Al (99.9999%) were used as reference specimens in CDB measurements.

A high resolution digital spectrometer [2] with a timing resolution of 150 ps (FWHM ^{22}Na) was employed for LT studies. At least 10^7 annihilation events were accumulated in each LT spectrum. The CDB spectrometer was equipped with two HPGe detectors and exhibits an overall energy resolution of 1.0 keV (FWHM) at 511 keV energy. At least 10^8 events were collected in each two-dimensional spectrum, which was subsequently reduced into one-dimensional Doppler profile and instrumental resolution cuts. The relative changes of Doppler profiles were followed as ratio curves of the Doppler profile normalized counts to those of the well annealed α-Fe reference profile. SPIS studies were performed on the magnetically guided variable energy positron beam "SPONSOR" [3]. The energy of incident positrons was varied in the range from 0.03 to 36 keV. The Doppler broadening of the annihilation line was measured by an HPGe detector with energy resolution of 1.09 ± 0.01 keV at 511 keV and evaluated in terms of the S parameter. Microhardness was examined by the Vickers method with a loading of 100 g applied for 10 s (HV0.1) using the STRUERS Duramin-2 micro-tester device.

Table 1 Summarized results of CDB, SPIS, and HV0.1 measurements: fraction of positrons annihilating with Al electrons obtained from fitting of CDB spectra using Eq. (4) (ξ_{Al}), positron diffusion length measured by SPIS (L_+), concentration of vacancies (c_v) determined by Eqs. (1) and (3).

specimen	ξ_{Al}	L_+ (nm)	c_v (at.$^{-1}$)	HV0.1
$Fe_{71.98}Al_{28.02}$	0.95(1)	4.0(2)	$5.0(5) \times 10^{-2}$ Eq. (3)	491(5)
$Fe_{75.99}Al_{24.01}$	0.89(1)	40(6)	$4.8(6) \times 10^{-4}$ Eq. (3)	412(5)
Fe_3Al	0.65(1)	90(10)	$7.3(5) \times 10^{-5}$ Eq. (1)	360(7)
			$7.0(8) \times 10^{-5}$ Eq. (3)	

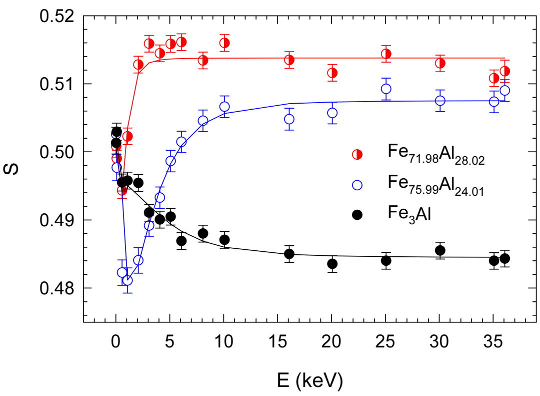

Figure 1 (Color online) The dependence of the S parameter on the energy E of incident positrons for the studied alloys. The curves fitted by VEPFIT are plotted by solid lines.

3 Results and discussion The dependence of the S parameter on positron energy measured by SPIS on quenched alloys is plotted in Fig. 1. A local minimum in $S(E)$ curves of non-stoichiometric alloys at low energies 1-2 keV is due to positron annihilations in a thin oxide layer formed on the surface during annealing. The $S(E)$ curves of these alloys were fitted by the VEPFIT [6] assuming two layers: (i) a thin oxide layer on surface, and (ii) the bulk alloy. On the other hand, the stoichiometric Fe_3Al alloy does not contain any oxide layer and was well-fitted by a single layer model. The positron diffusion lengths L_+ obtained from fitting are listed in Table 1. The Fe_3Al alloy exhibits the longest L_+ among the studied alloys and a remarkably lower S parameter than in the non-stoichiometric alloys. This testifies that Fe_3Al exhibits a lower concentration of quenched-in vacancies than the non-stoichiometric alloys, which is in accordance with the finding that the Fe_3Al alloy exhibits also the lowest hardness (See Table 1). Results of LT measurements for quenched alloys are listed in Table 2. The non-stoichiometric alloys exhibit a single component LT spectra with lifetimes significantly longer than the Fe_3Al bulk positron lifetime τ_B = 112 ps [4]. Thus virtually all positrons in these alloys are trapped at quenched-in vacancies (saturated trapping). On the other hand, the stoichiometric Fe_3Al alloy exhibits a two-component LT spectrum. The shorter component with a lifetime $\tau_1 < \tau_B$ comes from free positrons while the longer one with a lifetime τ_2 represents a contribution of positrons trapped in quenched-in vacancies. The concentration of quenched-in vacancies in the Fe_3Al specimen can be calculated using the two state simple trapping model (STM) [5]

$$c_v = \frac{1}{\nu_V}\frac{I_2}{I_1}\left(\frac{1}{\tau_B} - \frac{1}{\tau_2}\right), \tag{1}$$

where $\nu_v = 4 \times 10^{14}$ at.s^{-1} is the specific positron trapping rates for vacancies in Fe_3Al [4]. The concentration c_v of quenched-in vacancies in the Fe_3Al alloy obtained from Eq. (1) is given in Table 1. Note that the quantity τ_f=114(1) ps calculated from well-known equation

$$\tau_f = \left(\frac{I_1}{\tau_1} + \frac{I_2}{\tau_2}\right)^{-1}, \tag{2}$$

is in good agreement with τ_B testifying consistence of the decomposition of LT spectrum of Fe_3Al alloy with STM.

Table 2 Positron lifetimes and relative intensities resolved in LT spectra of studied alloys quenched from 1000 °C.

specimen	τ_1 (ps)	I_1 (%)	τ_2 (ps)	I_2 (%)
$Fe_{71.98}Al_{28.02}$	-	-	195.3(5)	100
$Fe_{75.99}Al_{24.01}$	-	-	190.8(4)	100
Fe_3Al	27(9)	10.5(6)	182.4(3)	89.5(8)

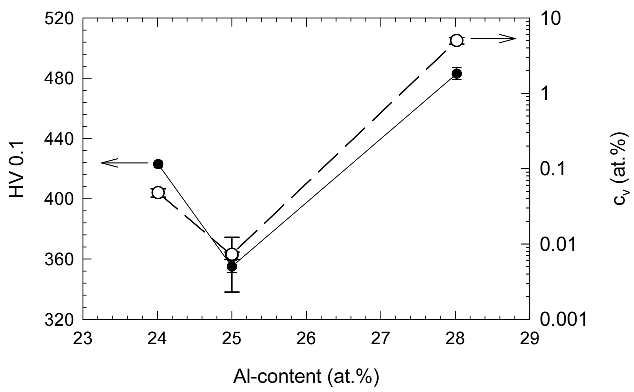

Figure 2 Microhardness HV0.1 (full symbols) and concentration of quenched-in vacancies c_v (open symbols) calculated from LT and SPIS results as a function of the Al content in studied alloys.

The concentration of quenched-in vacancies in non-stoichiometric alloys is definitely higher than in Fe_3Al. It cannot be calculated directly from LT results due to saturated trapping. However, positron trapping at vacancies causes a shortening of the positron diffusion length which is sensitive to changes of vacancy concentration even in the case of very high defect densities [7]. Hence, the concentration of quenched-in vacancies c_v can be determined from combination of SPIS and LT results using expression

$$c_v = \frac{1}{\nu_v \tau_B}\left(\frac{L_{+,B}^2}{L_+^2} - 1\right), \tag{3}$$

where $L_{+,B} \approx 180$ nm is the mean positron diffusion length in a defect-free Fe_3Al [7]. Concentrations of quenched-in vacancies c_v calculated using Eq. (3) are listed in Table 1 and plotted in Fig. 2 as a function of Al content. It is concluded that (i) stoichiometric Fe_3Al exhibits the lowest c_v among the studied alloys, (ii) non-stoichiometric alloys exhibits enhanced c_v which increases with the increasing Al-content, i.e. $Fe_{71.98}Al_{28.02}$ alloy exhibits the highest c_v, (iii) there is a clear correlation between c_v and HV0.1 testifying a hardening effect of quenched-in vacancies.

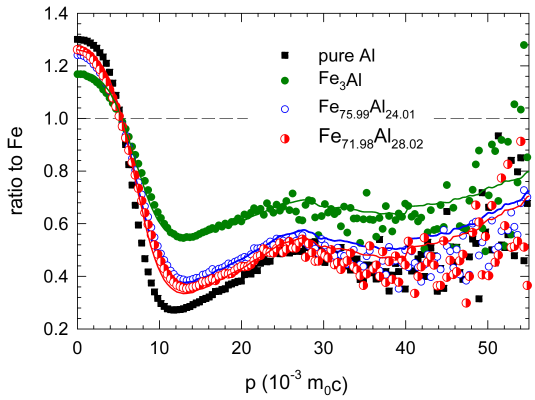

Figure 3 (Color online) The CDB ratio curves (related to well annealed pure Fe) for reference pure Al specimen and quenched Fe_3Al-based alloys. Solid lines show curves obtained from Eq (4) corresponding to Al fraction ξ_{Al} given for each alloy in Table 1.

The stoichiometric Fe_3Al alloy exhibits not only a lower c_v, but also a shorter lifetime τ_2 of positrons trapped in vacancies, see Table 2. This indicates that the nature of quenched-in vacancies in Fe_3Al differs from that in the non-stoichiometric alloys. From the first principles calculations, it is known that the formation energy of Al vacancies is significantly higher than that of the Fe vacancy [8]. Thus, it is expected that Fe_3Al-based alloys contain predominantly Fe-vacancies. The local chemical surrounding of Fe-vacancies depends on the sublattice where the vacancy is located and also on the degree of disorder (See [7] for more detailed discussion). It was found that the lifetime of positrons trapped in the Fe-vacancy increases with the increasing number of nearest neighbour Al atoms [7]. CDB investigations were performed to examine the chemical environment of quenched-in vacancies. The CDB ratio curves related to pure Fe are plotted in Fig. 3 together with a curve ρ_{Al} measured on a pure Al. The shape of the CDB curves is very similar to that of pure Al demonstrating that a significant fraction of positrons is annihilated by Al electrons. In the first approximation, the CDB ratio curve ρ for the studied alloys can be expressed as

$$\rho \approx \xi_{Al}\rho_{Al} + (1-\xi_{Al})\rho_{Fe}, \tag{4}$$

where ξ_{Al} is the fraction of positrons annihilating with Al electrons and $\rho_{Fe} = 1$. Solid lines in Fig. 3 show the best approximation of experimental curves by equation (4) and the fractions ξ_{Al} obtained from such fits are listed in Table 1. The non-stoichiometric alloys exhibit a high ξ_{Al}, which testifies that quenched-in vacancies are almost completely surrounded by Al atoms. Hence, CDB results proved that vacancies in these alloys are preferentially surrounded by Al atoms. On the other hand, the stoichiometric Fe_3Al exhibits remarkably lower ξ_{Al}. Quenched-in vacancies in Fe_3Al are, therefore surrounded by a smaller number of Al atoms, which is in agreement with shorter τ_2. The ξ_{Al} value obtained for Fe_3Al is not far from the value expected for Fe-vacancy in the Fe sublattice in the ordered $D0_3$ structure [7]. Hence, our results indicate that quenched Fe_3Al exhibits a higher degree of ordering than the non-stoichiometric alloys.

4 Conclusions

Stoichiometric Fe_3Al and non-stoichiometric $Fe_{75.99}Al_{24.01}$ and $Fe_{71.98}Al_{28.02}$ alloys quenched from 1000°C were studied. The non-stoichiometric alloys exhibit a higher concentration of quenched-in vacancies which increases with the Al content. Vacancies in these alloys are surrounded by Al atoms in the nearest neighbour sites. On the other hand, stoichiometric Fe_3Al exhibits a lower (but still significant) concentration of quenched-in vacancies which are on average surrounded by less number of Al atoms. This indicates a higher degree of ordering in the stoichiometric alloy.

Acknowledgements This work was supported by the Czech Scientific Foundation (contract No. GA106/08/P133) and by the Ministry of Education, Youths and Sports of the Czech Republic through the research plan No. MSM 0021620834.

References

[1] K. Ho and R.A. Dodd, Scr. Metall. **12**, 1055 (1978).
[2] F. Becvar, J. Cizek, I. Prochazka, and J. Janotova, Nucl. Instrum. Methods A **539**, 372 (2005).
[3] W. Anwand, H.-R. Kissener, and G. Brauer, Acta Phys. Polonica A **88**, 7 (1995).
[4] H.-E. Schaefer, R. Würschum, M. Sob, T. Zak, W.Z. Yu, W. Eckert, and F. Banhart, Phys. Rev. B **41**, 11869 (1990).
[5] P. Hautojärvi and C. Corbel, in: Positron Spectroscopy of Solids, edited by A. Dupasquier and A.P. Mills, Jr. (IOS, Amsterdam, 1995), p. 491.
[6] A. van Veen, H. Schut, M. Clement, J. de Nijs, and A. Kruseman, M. Ijpma, Appl. Surf. Sci. **85**, 216 (1995).
[7] O. Melikhova, J. Cizek, J. Kuriplach, I. Prochazka, M. Cieslar, W. Anwand, and G. Brauer, J. Phys.: Conf. Series (2009), in press.
[8] M. Fähnle, J. Mayer, and B. Meyer, Intermetallics **7**, 315 (1999).